INTERNATIONAL ATOMIC ENERGY AGENCY
UNITED NATIONS EDUCATIONAL, SCIENTIFIC AND CULTURAL ORGANIZATION

INTERNATIONAL CENTRE FOR THEORETICAL PHYSICS
34100 TRIESTE (ITALY) - P.O.B. 586 - MIRAMARE - STRADA COSTIERA 11 - TELEPHONE: 2240-1
CABLE: CENTRATOM - TELEX 460892-I

SMR/388- 27

SPRING COLLEGE IN MATERIALS SCIENCE
ON
'CERAMICS AND COMPOSITE MATERIALS'
(17 April - 26 May 1989)

HIGH TOUGHNESS AND HIGH TEMPERATURE CERAMICS

G. DUNLOP
Department of Physics
Chalmers University of Technology
412 96 Göteborg
Sweden

1989 ICTP Spring College in Materials Science

"Ceramics and Composite Materials"

HIGH TOUGHNESS AND HIGH TEMPERATURE CERAMICS

Gordon Dunlop

Department of Physics
Chalmers University of Technology
412 96 Göteborg
Sweden

May 1989

WHY CERAMICS
FOR STRUCTURAL PURPOSES ?

Because of their strong chemical bonding

covalent
covalent - ionic

many ceramic materials have a **high inherent strength**
and a **high melting temperature**

This leads to possibilities for the **development of rigid high strength materials with**

- high temperature strength
- high hardness
- wear resistance
- resistance to chemical attack
- low density
- special thermal properties
- special electrical properties

In practise have **problems** with:

- brittleness
  The materials have a high resistance to plastic deformation.
  Therefore difficult to relieve stress concentrations.
  - Low fracture toughness K_{Ic}
- high temperature strength
  - role of glassy phases inherited from liquid phase sintering
- high temperature oxidation
  - of nitrogen and carbide ceramics
  - role of glassy phases
- fabrication
  - forming, sintering
- machining
- joining

General references

M.H. Lewis, *Ceramics: applications and limitations* in Materials at their Limits, Inst of Metals, London, Book 392,1986.
M.V. Swain, *New developments and applications of engineering ceramics*, in Proc 1987 Conf. Inst Met Matls Australasia.

CERAMICS OF MAJOR INTEREST FOR STRUCTURAL APPLICATIONS

Al_2O_3

Si_3N_4

SiC

ZrO_2

(BN)

(TiB_2)

BASIC PROPERTIES

Comparitive data taken from
"Modern Ceramics Engineering" D. W. Richerson
Marcel Dekker, NY 1982

Density - low atomic weight, low coordination number, open structures

Melting temperatures - high

Thermal conductivity - generally lower than metals
Thermal expansion " " " "

Electrical resistivity - high

Elastic modulus - high

Strength:

$$\sigma_f = \frac{1}{Y} \frac{K_{Ic}}{\sqrt{c}}$$

-role of flaw sizes
fracture toughness

Thermal shock resistance
- thermal conductivity
- coeff. thermal expansion
- fracture toughness

Table 3.1 Typical Room-temperature Elastic Modulus Values for Important Engineering Materials

Material	Average elastic modulus, E	
	GPa	psi
Rubber	0.0035-3.5	5×10^2–5×10^5
Nylon	2.8	0.4×10^6
Polymethyl methacrylate	3.5	0.5×10^6
Urea-formaldehyde	10.4	1.5×10^6
Bulk graphite	6.9	1×10^6
Concrete	13.8	2×10^6
NaCl	44.2	6.4×10^6
Aluminum alloys	69	10×10^6
Fused SiO_2	69	10×10^6
Typical glass	69	10×10^6
ZrO_2	138	20×10^6
Mullite ($Al_6Si_2O_{13}$)	145	21×10^6
UO_2	173	25×10^6
Iron	197	28.5×10^6
MgO	207	30×10^6
Ni-base superalloy (IN-100)	210	30.4×10^6
Spinel ($MgAl_2O_4$)	284	36×10^6
Si_3N_4	304	44×10^6
BeO	311	45×10^6
Al_2O_3	380	55×10^6
SiC	414	60×10^6
TiC	462	67×10^6
Diamond	1035	150×10^6

Source: Data from Refs. 6, 7, and 8.

3.1

YOUNG'S MODULUS OF ELASTICITY E (psi)

Figu

F
ous
cres
ther
nece
M
of m
Inte
are
orga
(ma
mod

Table 2.1 Specific Gravity of Ceramic, Metallic, and Organic Materials

Material	Composition	Density (g/cm^3)
	Ceramic materials	
α-Aluminum oxide	α-Al_2O_3	3.95
γ-Aluminum oxide	γ-Al_2O_3	3.47
Aluminum nitride	AlN	3.26
Mullite	$Al_6Si_2O_{13}$	3.23
Boron carbide	B_4C	2.51
Boron nitride	BN	2.20
Beryllium oxide	BeO	3.06
Barium titanate	$BaTiO_3$	5.80
Diamond	C	3.52
Graphite	C	2.1-2.3
Fluorite	CaF_2	3.18
Cerium oxide	CeO_2	7.30
Chromium oxide	Cr_2O_3	5.21
Spinel	$MgAl_2O_4$	3.55
Iron aluminum spinel	$FeAl_2O_4$	4.20
Magnetite	$FeFe_2O_4$	5.20
Hafnium oxide	HfO_2	9.68
Spodumene	$LiAlSi_2O_6$	3.20
Cordierite	$Mg_2Al_4Si_5O_{18}$	2.65
Magnesium oxide	MgO	3.75
Forsterite	Mg_2SiO_4	3.20
Quartz	SiO_2	2.65
Tridymite	SiO_2	2.27
Cristobalite	SiO_2	2.32
Silicon carbide	SiC	3.17
Silicon nitride	Si_3N_4	3.19

Table 2.1 (continued)

Material	Composition	Density (g/cm^3)
Titanium dioxide	TiO_2	4.26
Tungsten carbide	WC	15.70
Zirconium oxide	ZrO_2	5.80
Zircon	$ZrSiO_4$	4.65
	Metals	
Aluminum	Al	2.7
Iron	Fe	7.87
Magnesium	Mg	1.74
1040 Steel	Fe-base alloy	7.85
Hastelloy X	Ni-base alloy	8.23
HS-25 (L605)	Co-base alloy	9.13
Brass	70 Cu-30 Zn	8.5
Bronze	95 Cu-5 Sn	8.8
Silver	Ag	10.4
Tungsten	W	19.4
	Organic materials	
Polystyrene	Styrene polymer	1.05
Teflon	Polytetrafluoroethylene	2.2
Plexiglass	Polymethyl methacrylate	1.2
Polyethylene	Ethylene polymer	0.9

Society for Testing and Materials Specification ASTM C373 [1]. The latter technique permits direct measurement of bulk density, open porosity, water absorption, and apparent specific gravity and indirect assessment of closed porosity. The procedure involves first measuring the dry weight (D). The part is then boiled in water for 5 hr and then allowed to cool in the water for 24 hr. The wet weight in air W and the wet weight suspended in water S are then measured. The following can then be calculated:

Table 2.2 Melting Temperatures of Ceramic, Metallic, and Organic Materials

Material	Approximate melting temperature	
	°C	°F
Polystyrene (GP grade)	65–75	150–170[a]
Polymethyl methacrylate	60–90	140–200[a]
Na metal	98	208
Polyethylene	120	250[a]
Nylon 6[b]	135–150	275–300[a]
Polyimides	260	500[a]
Teflon	290	550[a]
B_2O_3	460	860
Al metal	660	1220
NaCl	801	1474
Ni-base superalloy (Hastelloy X)	1300	~2370
Co-base superalloy (Haynes 25)	1330–1410	2425–2570
Stainless steel (304)	1400–1450	2550–2650
CaF_2		
Fused SiO_2	~1650	3000
Si_3N_4[b]	~1750–1900	3180–3450
Mullite	1850	3360
Al_2O_3	2050	3720
Spinel	2135	3875
B_4C	2425	4220
SiC[b]	2300–2500	4170–4530
BeO	2570	4660
ZrO_2 (stabilized	2500–2600	4530–4710
MgO	2620	4750
WC	2775	5030
UO_2	2800	5070
TiC	3100	5520
ThO_2	3300	5880
W metal	3370	6010
C[a]	3500	6240
HfC	3890	6940

[a] Maximum temperature for continuous use.
[b] Sublimes.

Table 3.5 Typical Room Temperature Strengths of Ceramic Materials

Material	MOR		Tensile	
	MPa	kpsi	MPa	kpsi
Sapphire (single-crystal Al_2O_3)	620	90	--	--
Al_2O_3 (0-2% porosity)	350-580	50-80	200-310	30-45
Sintered Al_2O_3 (<5% porosity)	200-350	30-50	--	--
Alumina porcelain (90-95% Al_2O_3)	275-350	40-50	172-240	25-35
Sintered BeO (3.5% porosity)	172-275	25-40	90-133	13-20
Sintered MgO (<5% porosity)	100	15	--	--
Sintered stabilized ZrO_2 (<5% porosity)	138-240	20-35	138	20
Sintered mullite (<5% porosity)	175	25	100	15
Sintered spinel (<5% porosity)	83-220	12-32	--	19
Hot-pressed Si_3N_4 (<1% porosity)	620-965	90-140	350-580	50-80
Sintered Si_3N_4 (~5% porosity)	414-580	60-80	--	--
Reaction-bonded Si_3N_4 (15-25% porosity)	200-350	30-50	100-200	15-30
Hot-pressed SiC (<1% porosity)	621-825	90-120	--	--
Sintered SiC (~2% porosity)	450-520	65-75	--	--
Reaction-sintered SiC (10-15% free Si)	240-450	35-65	--	--
Bonded SiC (~20% porosity)	14	2	--	--

Table 3.5 (continued)

Material	MOR		Tensile	
	MPa	kpsi	MPa	kpsi
Fused SiO_2	110	16	69	10
Vycor or Pyrex glass	69	10	--	--
Glass-ceramic	245	10-35	--	--
Machinable glass-ceramic	100	15	--	--
Hot-pressed BN (<5% porosity)	48-100	7-15	--	--
Hot-pressed B_4C (<5% porosity)	310-350	45-50	--	--
Hot-pressed TiC (<2% porosity)	275-450	40-65	240-275	35-40
Sintered WC (2% porosity)	790-825	115-120	--	--
Mullite porcelain	69	10	--	--
Steatite porcelain	138	20	--	--
Fire-clay brick	5.2	0.75	--	--
Magnesite brick	28	4	--	--
Insulating firebrick (80-85% porosity)	0.28	0.04	--	--
2600°F insulating firebrick (75% porosity)	1.4	0.2	--	--
3000°F insulating firebrick (60% porosity)	2	0.3	--	--
Graphite (grade ATJ)	28	4	12	1.8

Mode I is most frequently encountered for ceramic materials. Stress analysis solutions for K_I for a variety of crack locations within simple geometries have been reported by Paris and Sih [25]. Experimental data for a variety of materials have been obtained for the critical stress intensity K_{I_C}. This is the stress intensity factor at which the crack will propagate and lead to fracture. It is also referred to as fracture toughness and is

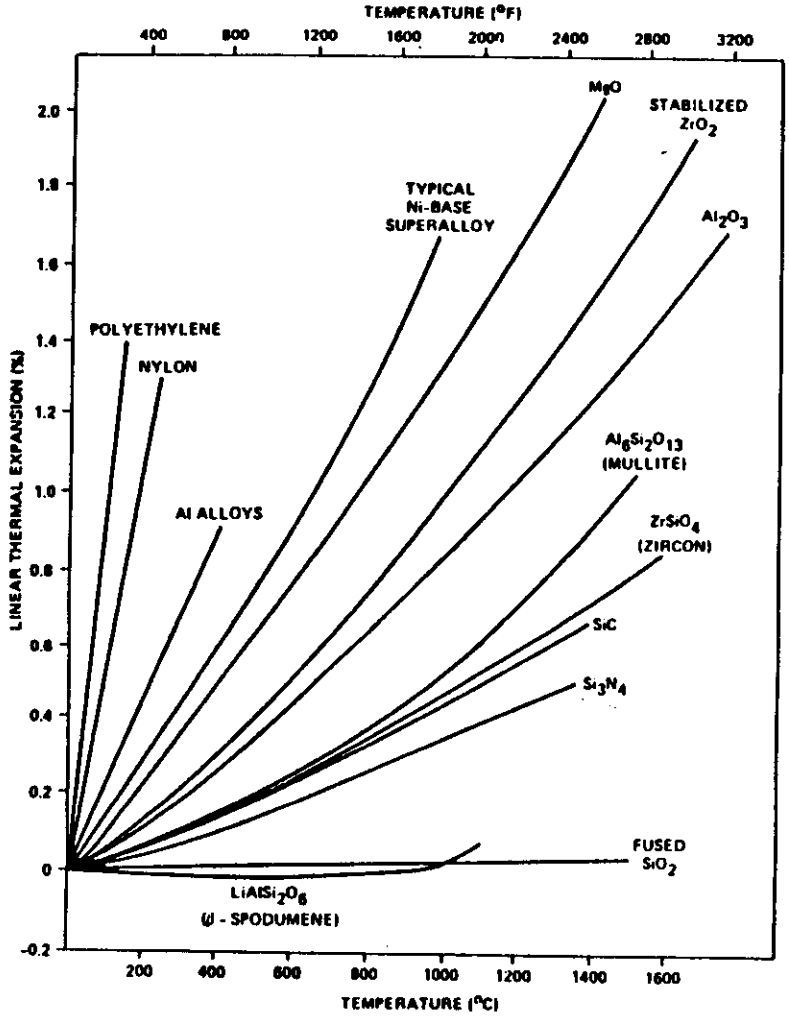

Figure 2.3 Thermal expansion characteristics of typical metals, polymers, and polycrystalline ceramics (from numerous sources.)

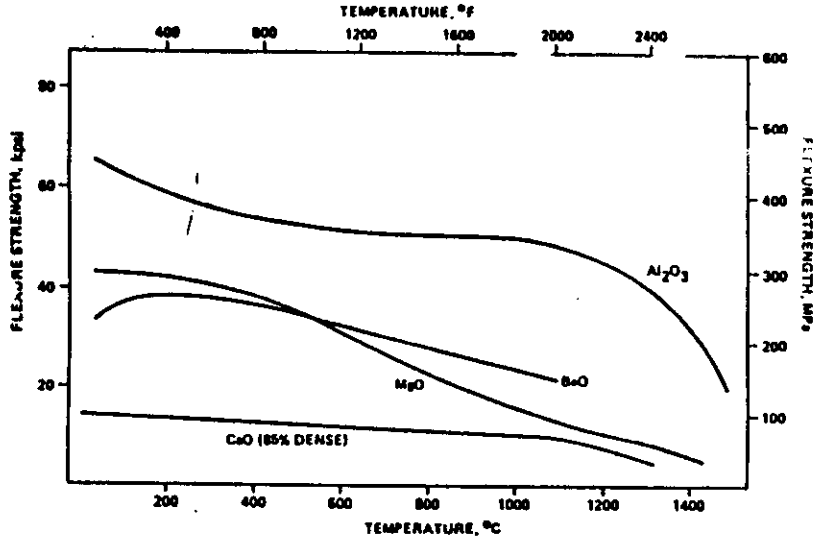

Figure 3.11 Strength versus temperature for oxide and silicate ceramics.

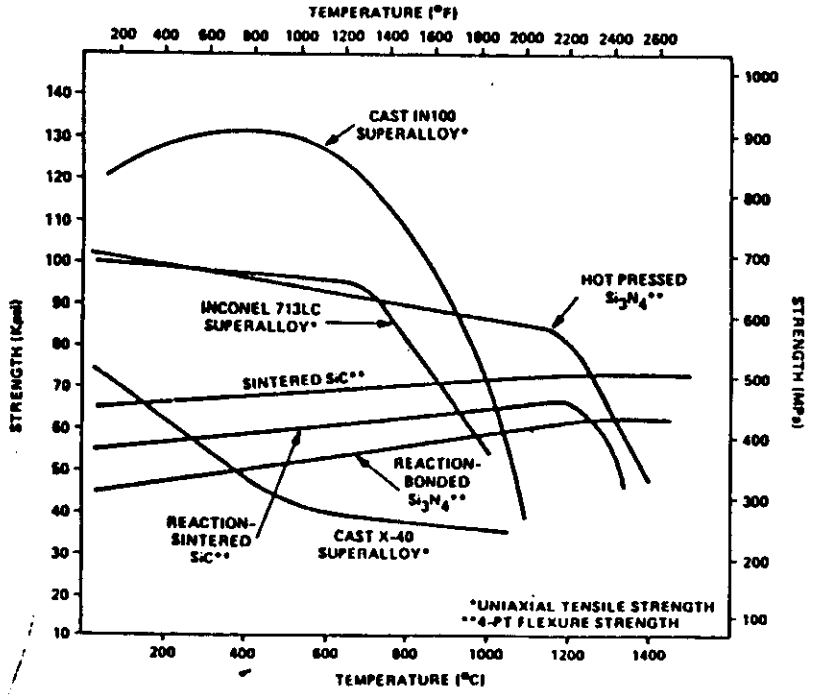

Figure 3.12 Strength versus temperature for carbide and nitride ceramics and superalloy metals.

APPLICATIONS OF HIGH PERFORMANCE CERAMICS

Heat engines
- gas turbines
- piston engines

Nozzles, seals
- metallurgical industry
- chemical industry
- household plumbing
- face seals at rotating interfaces

Armour plate
- composite, light weight armour

Biomaterials
- limbs, joints, teeth

Wear parts
- bearings

Machine tools
- cutting tools
- dies for extrusion
- knives

High temperature heat exchangers

	specific stiffness E/ρ	melting / decomposition T C
AlN	4	2450
Al_2O_3	3	2050
SiC	6	2600
Si_3N_3	4	1900
steel	1	1400 - 1500
Al	1	660

THE MICROSTRUCTURE OF HIGH PERFORMANCE CERAMICS

General

The microstructure is a product of fabrication processes

- raw materials
- powder technology
  - grinding
  - mixing
  - colloid chemistry
- sintering aids
  - liquid phase sintering
- forming process
  - cold pressing
  - slip casting
  - injection moulding (burn off problem)
- sintering
  - pressureless
  - hot pressing
  - hot isostatic pressing
- thermal history
  - heat treatment

Fabrication variables determine microstructure

- compositions
  - micro and macro
- grain morphologies, sizes and size distributions
- glassy phases
  - volume and composition
- secondary crystalline phases

Silicon nitride Si_3N_4

Two polymorphs

α,β

both hexagonal crystal structure with difference in stacking sequence

α ABCDABCD—

β ABAB—

α - Si_3N_4 generally forms by vapour phase reaction

β - Si_3N_4 forms by liquid phase reaction

unit cell dimensions:

structure	a (Å)	c (Å)	ρ (g/cm³)
α - Si_3N_4	7.748	5.617	3.183
β - Si_3N_4	7.608	2.911	3.192

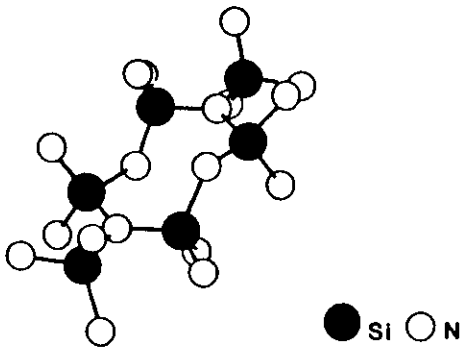

Fig. 3.1: The β - Si_3N_4 structure that is built up by corner sharing SiN_4 tetrahedra (ref. reference (55).

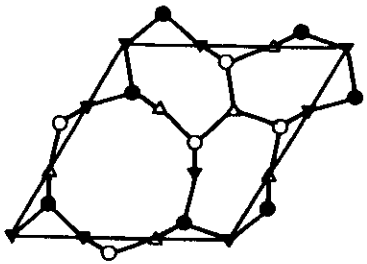

▼N ●Si layer A

△N ○Si layer B

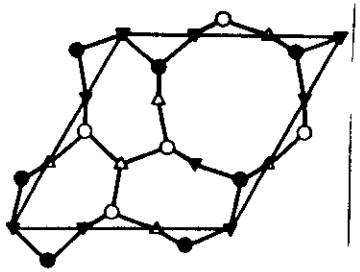

▼N ●Si layer C

△N ○Si layer D

Liquid phase sintering of Si_3N_4

Liquid phase is neccessary for densification because of:

- low diffusivity
- protective oxide layer on Si_3N_4 particles

Solution - precipitation reaction:

$$\alpha\text{-}Si_3N_4 + SiO_2 + MO \xrightarrow{1800\,^\circ C} \beta\text{-}Si_3N_4 + M\text{-}Si\text{-}O\text{-}N$$

surface additive — glass phase

Common additives

MgO

*Y_2O_3 (+ Al_2O_3)

Sc_2O_3

Additives react with $Si_3N_4 + SiO_2$ to form a low melting liquid

- this liquid generally forms a glass on cooling
- possibility of forming secondary crystalline phases during slow cooling or heat treatment

Fig. 2. Jänecke composition prism for the Y-Si-Al-O-N system. The compositions marked A-E cover the region investigated and represent additions of up to 20wt% Si_3N_4.

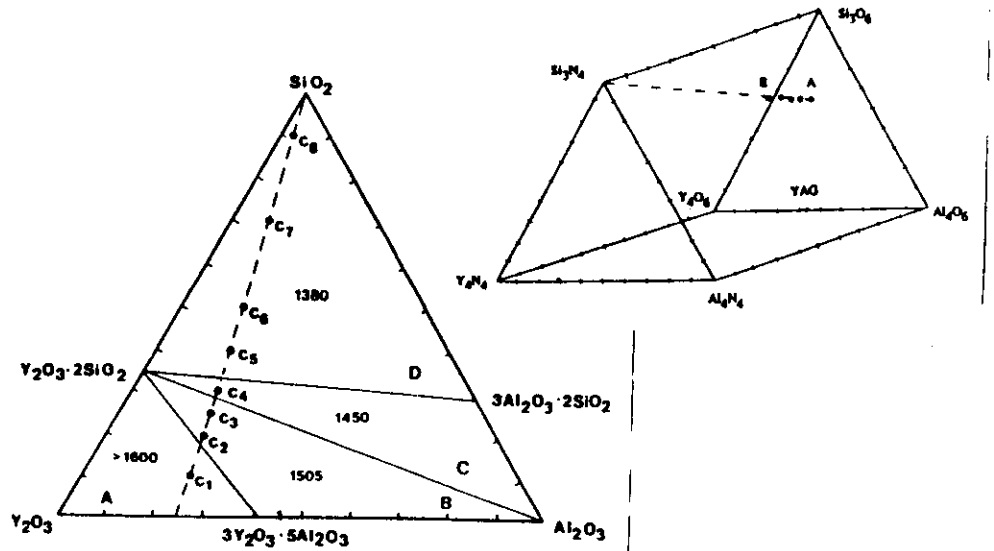

Fig. 1. Experimental behaviour diagram for the Y_2O_3-Al_2O_3-SiO_2 system. Compositions of the specimens which were investigated are indicated as also are the experimentally determined eutectic temperatures.

SiAlON

$$\alpha\text{–}Si_3N_4 + SiO_2 + AlN + MO \xrightarrow{1800^\circ C} \beta'\text{–}Si_{3-x}Al_xO_xN_{4-x} + \text{M-Si-Al-O-N glass phase}$$

surface additives

Solution of balanced amounts of Al & O in β–Si_3N_4 lattice

Considerable solid solution is possible.

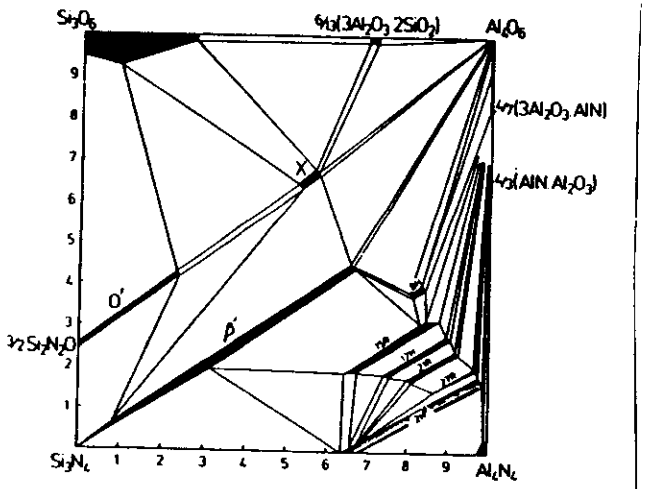

Fig. 3.7: Behaviour diagram for the system Si_3N_4-SiO_2-Al_2O_3-AlN at 1750 °C, after reference (77).

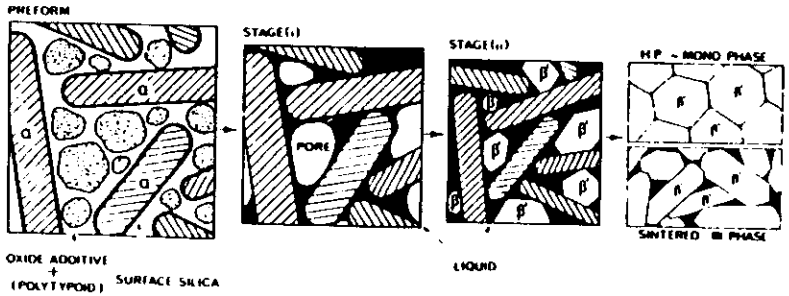

Fig. 4. Sintering reactions and the evolution of microstructure for HPSN and SSN ceramics.

Silicon carbide Si C

α–SiC - hexagonal
β–SiC -cubic

SiC has -high strength
-better high temperature strength - than Si_3N_4
-poorer fracture toughness - than Si_3N_4
-poorer thermal shock resistance - than Si_3N_4

Sintering additives

B + C - removal of SiO_2 on SiC powders via C
- catalysis of surface/ gb diffusion via B

Al / Al_2O_3
- leaves alumino silicate residues at gbs - softens at 1200 C
- poor high temperature properties

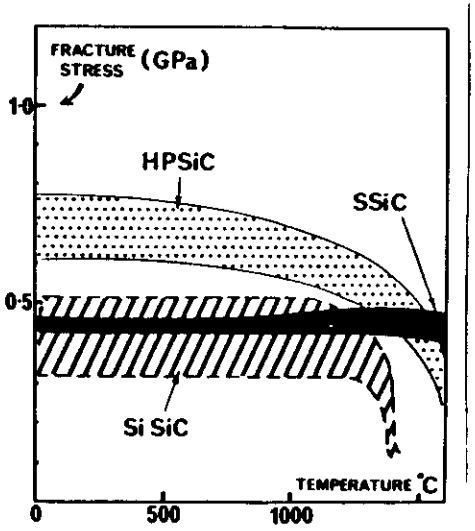

Fig.12. Bend strength (MOR) - temperature relationships for various SiC-based ceramics (~~see table 555~~).

Zirconia ZrO_2

Ref: R. Stevens, Magnesium Elektron Publication No. 113

Primarily ionic bonding

Three polymorphs of pure ZrO_2:

monoclinic 1170 °C tetragonal 2370 °C cubic 2680 °C liquid

Influence of "stabilising" additions eg. MgO, Y_2O_3, CaO

- extension of cubic and tetragonal phase fields to lower transformation temperatures

PHASE DIAGRAMS:

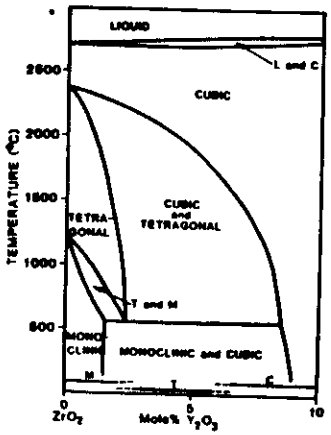

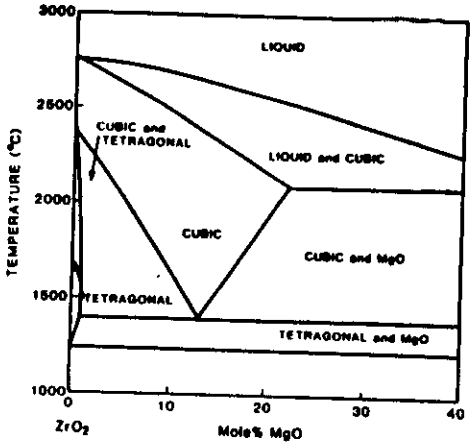

Sintering of ZrO_2

ZrO_2 is relatively soft at sintering temperatures 1400 - 1500 °C
- ionic bonding

Always have liquid phase present during sintering (small volume fraction).
Usually no intentional addition of sintering aids.

Tetragonal - monoclinic transformation

- martensitic
diffusionless shear process, near sonic velocities

- cf. iron base alloys "ceramic steel"

- volume expansion m → t ~ 5%

This transformation is the basis of *transformation toughened ceramics*

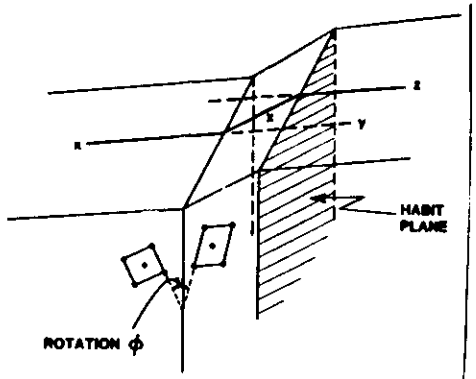

FIGURE 7. Schematic representation of a martensitic invariant plane strain transformation showing the surface tilting, scratch displacement, and total lattice strain associated with the transformation.

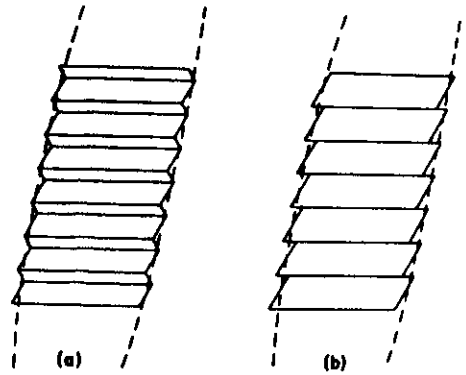

FIGURE 8. Schematic illustration of (a) internally twinned and (b) internally slipped martensitic plates. Such deformations ensure that the interface plane prevents the accumulation of strain and remains macroscopically undistorted. (After Wayman, C. M., *Introduction to the Crystallography of Martensitic Transformations*, MacMillan, New York, 1965.)

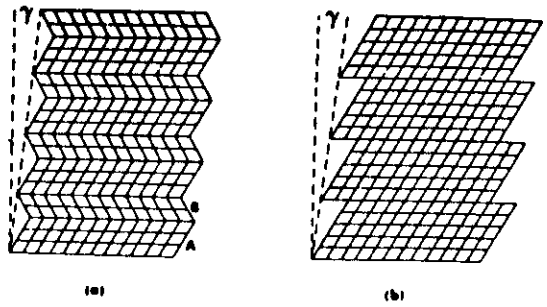

FIGURE 9. Schematic illustration of how slip and twinning may accomplish the same magnitude of inhomogeneous shear (angle γ)

TZP - tetagonal zirconia polycrystals

- low solute oxide additions - generally 2-4 mol% Y_2O_3
- sintered in the tetragonal single phase field
  1350-1500 °C

For stabilisation of t phase to lower temperatures
- grain size < critical size
  usually g.s. = 0.2 - 1 μm

Residual intergranular glass phase
- impurity silicates, Al_2O_3 & Y_2O_3 additions
- pick-up of Si etc from ball mills
provides liquid phase sintering medium

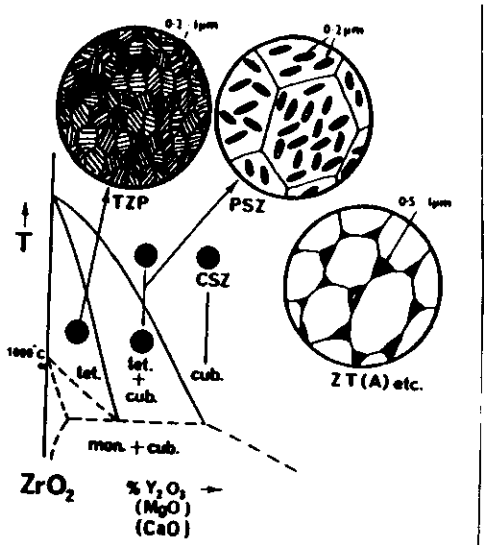

Fig.13. Phase equilibria and related microstructures for ZrO_2-toughened ceramics.

PSZ - partially stabilised zirconia

- alloyed with 8-10 mol % MgO, CaO, Y_2O_3.

- sintered in cubic phase field 1650-1850 °C
  - produces large (ca. 100μm) cubic grains

- cooled and heat treated in t+c phase field 1100-1450 °C
  - coherent precipitates of t in c matrix

- time & temp of heat treatment is critical to development of appropriate size precipitates

small precipitates
(0.2μm) are constrained and do not transform to m
- except in tensile stress field
  eg. at tip of propagating crack

large precipitates
transform to m on cooling and cannot then participate in transfomation toughening.

- if precipitates are *too small* - then might not transform in stress field and therefore will not participate in transformation toughening either.

Two phase zirconia toughened ceramics

ZTA zirconia toughened alumina

Tetragonal stabilised zirconia can be dispersed in other ceramic matrices

- grain size of t-ZrO_2 is critical for thermal stability
  (eg. stability to room temperature)
  - and fracture toughening.

- typically in 0.2-1 μm range depending upon matrix and impurity levels.

critical grain size for t-ZrO_2 is ~ 0.5μm
- in Al_2O_3 with 0.5-5 μm grain size

SOME COMPARITIVE PROPERTIES

(Magnesium Elektron Ltd Publ. no. 113)

	σ_f (MPa)	K_{Ic} ($MNm^{3/2}$)
MgO PSZ	600	9
CaO PSZ	650	6.6
Y_2O_3 PSZ	650	6.4
ZTA (25 vol% Al_2O_3)	1200	15
SiAlON + 25 vol% ZrO_2	950	8.5
TZP	880-1275	7.9-9.4

STRONG TOUGH CERAMICS

Refs:

1. R. W. Rice "Capabilities and design issues for emerging tough ceramics" Ceram Bull. 63, 1984, (2), 256.

2. F.F. Lange "Powder processing science and technology for increased reliability" J. Amer. Ceram. Soc, 72, 1989, 3-15.

3. F.F. Lange et al. "Processing related fracture origins: I, II, III" J. Amer. Ceram. Soc, 66, 1983, 396-408.

Fracture strength given by:

$$\sigma_f = \frac{1}{Y} \frac{K_{Ic}}{\sqrt{c}}$$

Improve strength by

- increased toughness, K_{Ic}
- decreased flaw size, c.

Flaw size approach to improved reliability
eg Rice:

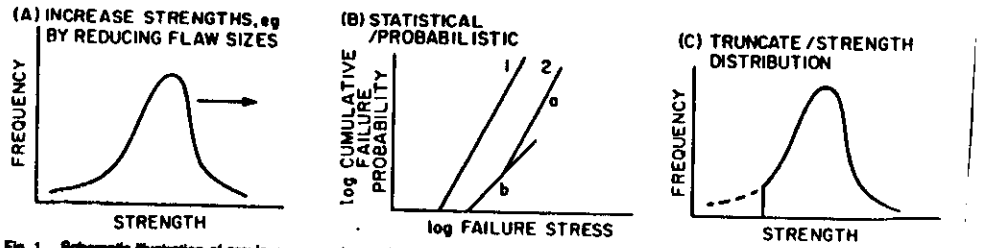

Fig. 1. Schematic illustration of previous approaches to improving the reliability of structural ceramics. (A) Illustrates the oldest approach of improving the strengths illustrated here by showing a shift of the strength distribution to higher strength levels as typically measured by the improvements in medium or average strengths; (B) illustrates the statistical probabilistic approach wherein the strength distribution is better defined in order to predict the probability of failure at any given stress level for a population of specimens or components; and (C) illustrates the approach of truncating the lower end of the strength distribution by either proof testing or nondestructive (NDE).

Flaws: - Largest flaw provides the weakest link.
Flaws introduced by:

raw materials
powder processing
extraneous particulates
drying
burn out of polymeric binders
differential sintering of agglomerates
surface machining

Introduction of flaws during powder processing steps:

Ref. F.F. Lange J. Amer. Ceram. Soc, 72, 1989, 3-15.

1. Powder manufacture
2. Powder preparation
3. Consolidation to shape
4. Densification / microstructural development

Each step can introduce an heterogeneity which can persist, or develop further, into the finished product.

Identify heterogeneities by fractography
- generally small number / unit vol. and difficult to find by other means

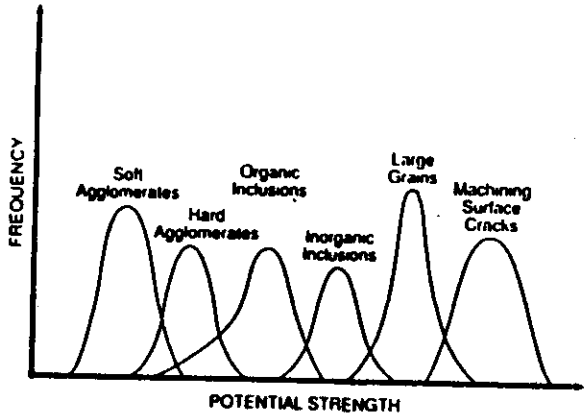

Fig. 1. Schematic plot of frequency versus potential strength of different flaw populations potentially present in a ceramic material. Frequency distribution and ordering depends on processing method and material characteristics.

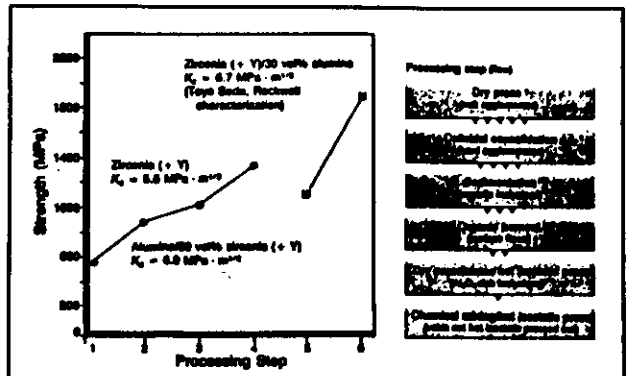

Changes in processing directed by the need to eliminate stress-concentrating heterogeneities found at fracture origins can significantly increase the mean strength of three transformation-toughened ceramics. Systematic strengthening was accomplished by first relating the flaws observed at fracture origins with a processing step. Processing changes were implemented to either eliminate the heterogeneity or reduce its size to result in an incremental strengthening. A less detrimental flaw population was then uncovered, identified, associated with a processing step, and eliminated with another change in processing. Sequential strengthening was achieved with this iterative scheme. Colloidal treatment of powders, which broke apart large, weak agglomerates and fractionated larger, strong agglomerates, and slurry consolidation played a major role in the processing changes that resulted in significant strengthening.

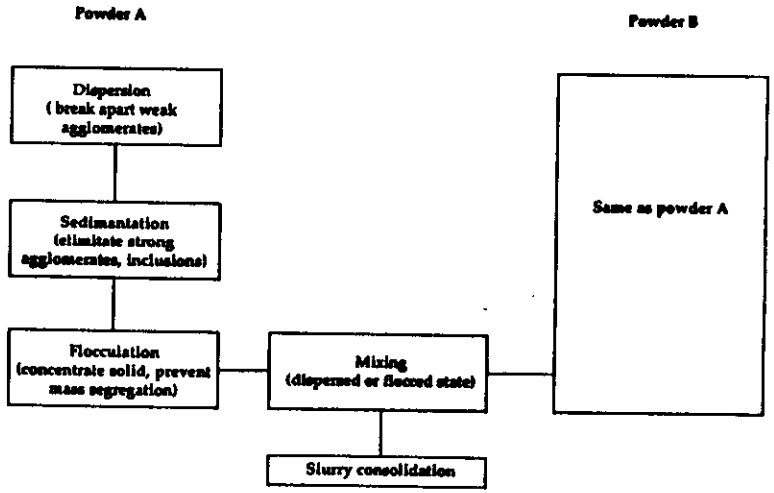

Fig. 2. One colloidal method for breaking apart weak agglomerates and fractionating desired particles from unwanted hard agglomerates and inclusions. Each powder in a multiphase system is treated the same before mixing.[7]

IMPROVING FRACTURE TOUGHNESS

Main approaches:

microcracking
residual stresses
crack bridging
crack deflection
* transformation toughening
* whisker reinforcement
* fibre reinforcement

Historical trends in improving toughness and strength

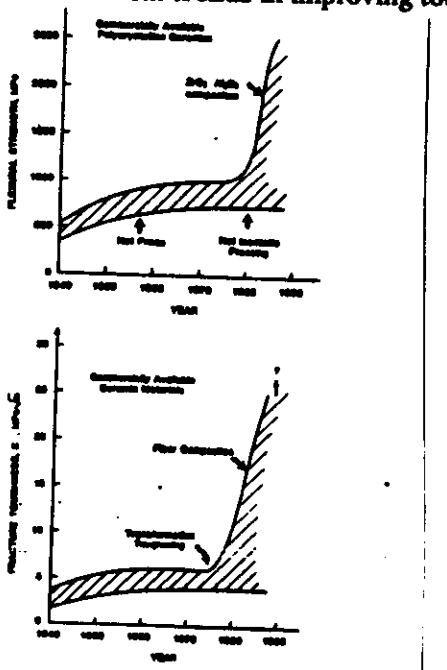

Figure 1. Historical trend of the fracture toughness and strength of commercially available ceramic materials.

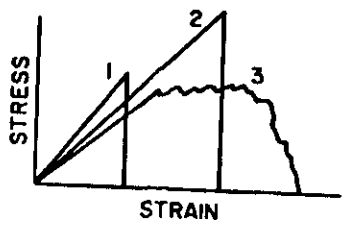

Fig. 4. Schematic illustration of the approaches to developing new tougher ceramics. Curve 1 illustrates the usual catastrophic failure of traditional ceramics, i.e., the material reaches its ultimate load-carrying capability and fails catastrophically so that the load-carrying capability drops essentially instantaneously to zero. Curve 2 shows the type of load deflection or stress strain curve common for particulate composites wherein catastrophic failure still occurs; however, toughness is increased, as for example reflected by the area under the stress strain curve and frequently exhibiting a lower Young's modulus and hence greater strain to failure. This may occur with decreased, the same, or higher strength than the matrix material, depending on a variety of factors. Curve 3 illustrates the type of behavior characteristic of ceramic fiber composites, at least those with continuous fibers, wherein the toughness is increased, as reflected by the area under the low deflection or stress strain curve and equally or more important the material maintains substantial load-carrying capability past its peak load.

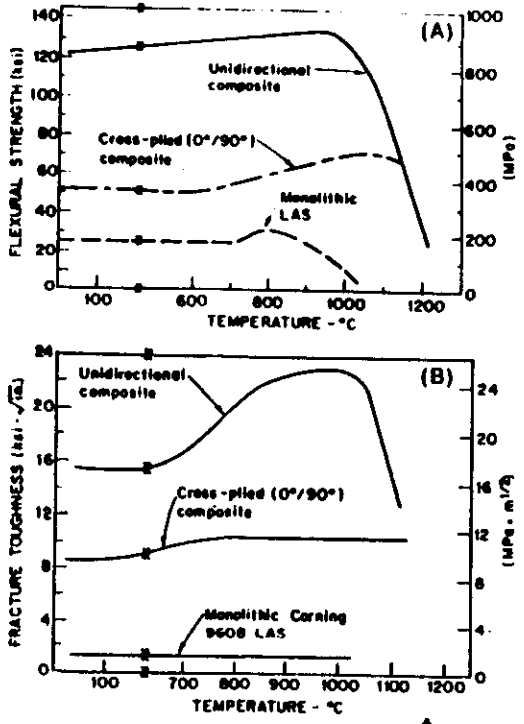

Fig. 7. Illustrative temperature capabilities of ceramic fiber composites. (A) strength; and (B) fracture toughness of a composite using SiC fibers and a lithium aluminum silicate crystallized glass matrix (after work of Dr. Karl Prewo and colleagues of United Technology Research Center).

TRANSFORMATION TOUGHENING

eg. TZP, PSZ

Ref: D.J. Green, R.H.J. Hannink & M.V. Swain "Transformation toughening of ceramics" CRC Press, 1989

Basis:

Volume increase ~ 5%

ZrO_2 , t → m phase transformation

Material contains constrained, untransformed precipitates / grains

Crack frontal zone

tensile stresses at crack tip decrease constraint

→ transformation

this somewhat reduces stress intensity at crack tip

- crack tip shielding

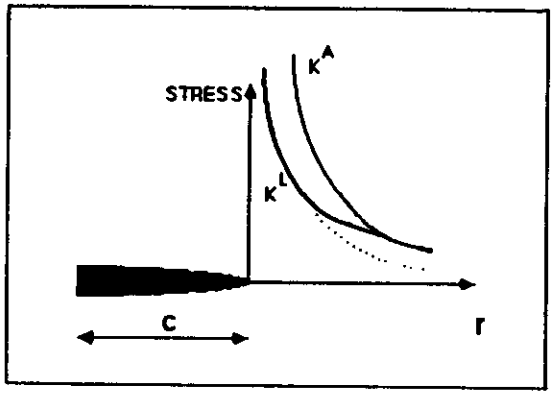

FIGURE 8. In crack-tip shielding, the stresses near a crack tip are reduced locally, so their magnitude is described by a local stress-intensity factor (K_T^+) rather than the applied value (K_T^+).

Steady state zone

Transformed particles in wake of crack tip exert closure stresses on crack

$$\Delta K_{IC} = 0.2143\, E\, V\, e^T\, h^{1/2} / (1-\nu)$$

E elastic modulus
V vol fraction transforming precipitates
e^T dilational strain due to transformation
h width of transformed zone
ν Poisson's ratio

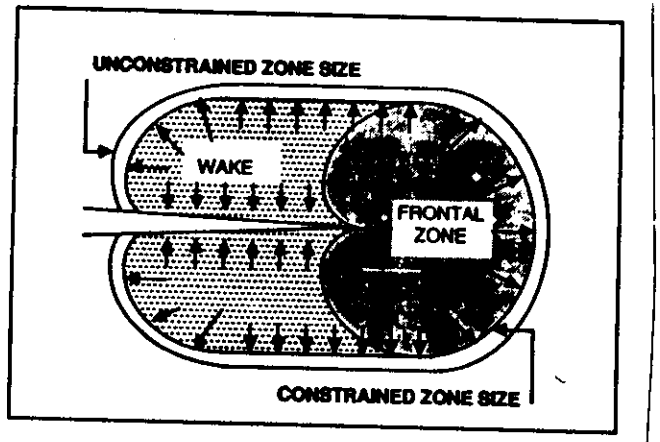

FIGURE 12. A representation of the stresses that arise in a dilatant transformation zone. The zone must be reduced in size from its unconstrained size to fit in the untransformed material. Once the zone extends behind the crack tip, stresses in the zone arise that are acting in a direction to close the crack.

this leads to R curve behaviour

R - curve behaviour

Resistance to crack growth increases as crack extends

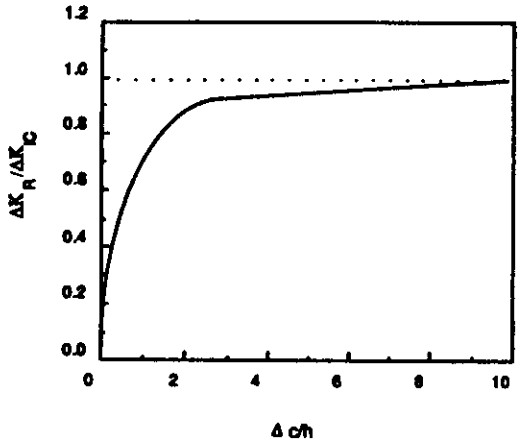

FIGURE 13. The toughening increase (ΔK_R), normalized by its asymptotic value (ΔK_{IC}), that occurs as a crack extends, such that the transformation zone is left behind the crack tip. (After McMeeking, R. and Evans, A. G., *J. Am. Ceram. Soc.*, 65, 242, 1982.)

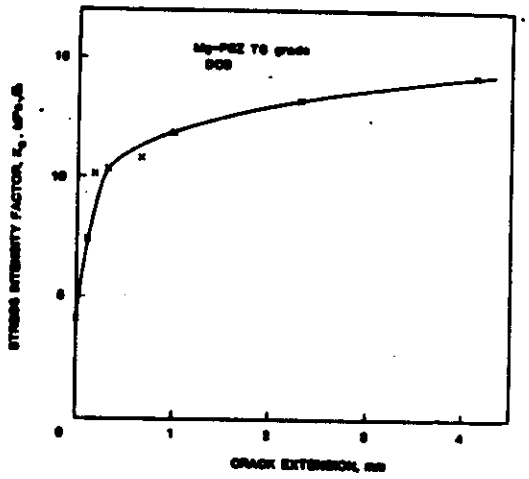

Figure 7. Observed R-curves in transformation toughened ceramics.

Effect of particle size and volume fraction:

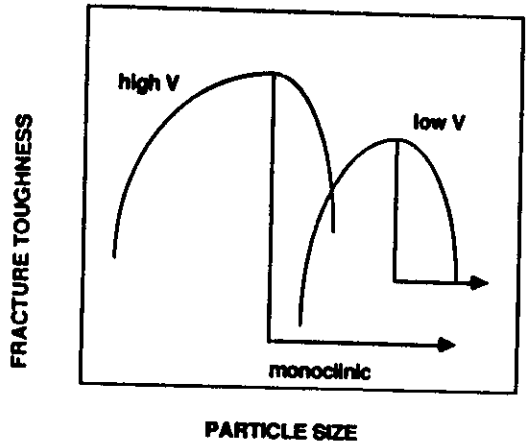

FIGURE 19. Effect of particle size and volume fraction of zirconia on fracture toughness.

Effect of temperature and solute additions:

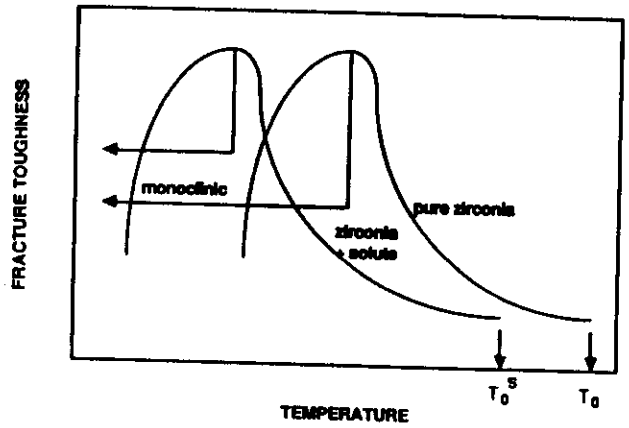

FIGURE 18. Schematic of the effect of temperature changes and solute addition on the fracture toughness of a transformation-toughened material. The toughness increases with decreasing temperature until the t-ZrO_2 can no longer be retained.

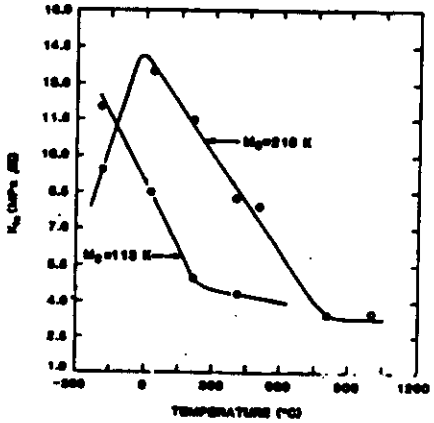

Figure 6. Temperature dependences of the toughness of Mg-PSZ materials.

MICROCRACK TOUGHENING

Cracking due to localised residual stresses from:

- phase transformations
- thermal expansion anisotropy - single phase materials
- thermal expansion, elastic mismatch
- multiphase materials

(a) *Spontaneous formation of microcracks during fabrication*
- particle size > critical size

toughening by crack tip bifurcation

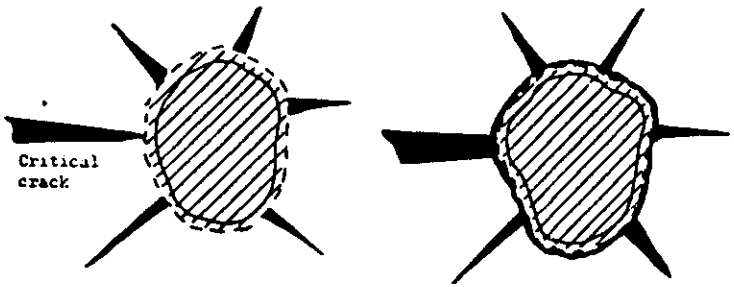

Figure (20) The martensitic transformation that occurs in ZrO_2 (tetragonal to monoclinic at 900-1100°C) with its 3-5% volume expansion, develops microcracks around the ZrO_2 particles (a). A crack propagating into the particle is deviated and becomes bifurcated (b), thus increasing the measured fracture resistance.

This mechanism gives significant toughness increase but generally little increase in strength

- microcracks are likely failure origins

(b) *Formation of microcracks in crack frontal zone*

→ crack tip shielding

eg, ZTA, overaged PSZ

Particle size < critical size for spontaneous cracking during fabrication

~ 0.5 critical size for spontaneous cracking

Shielding effects

-- dilation due to cracking

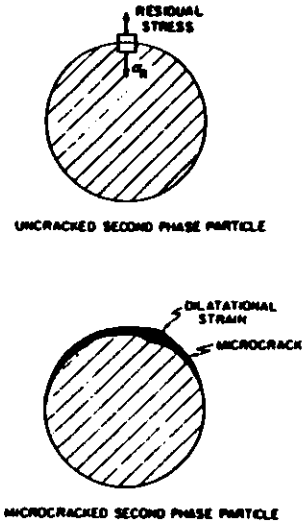

Fig. 8. A schematic showing the dilatation that accompanies microcracking, following relief of a residual tension.

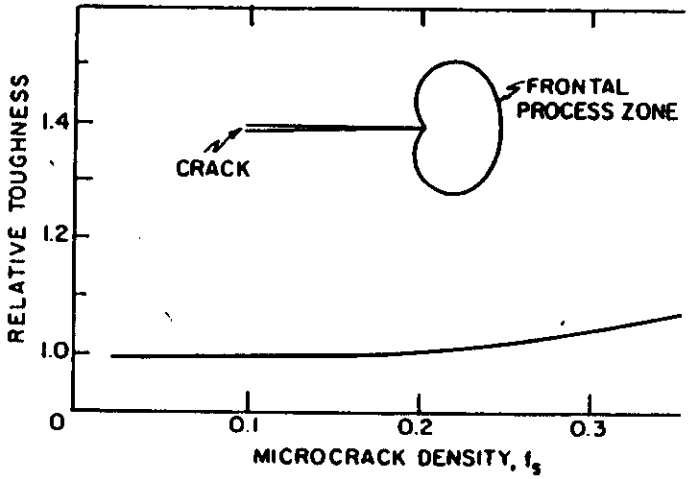

Fig. 9. Effects of a frontal microcrack process zone on toughening.

As for transformation toughening, effect of frontal zone on ΔK_{IC} is small.
Presence of process zone wake enhances toughness. Therefore get R-curve.
Evans:

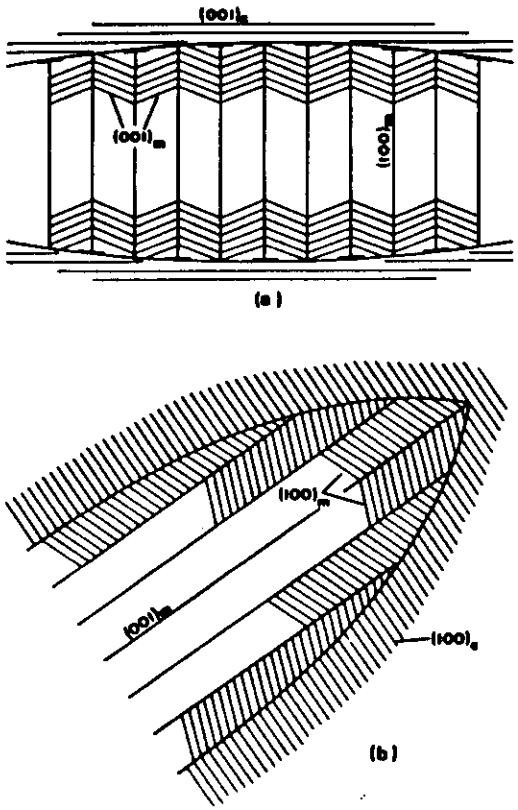

FIGURE 16. Schematic representation of lattice displacements developed at the particle matrix interface as a result of the tetragonal to monoclinic transformation. Particles have twin variant boundaries parallel to (a) $(100)_m$ planes and (b) $(001)_m$ planes. Positions of maximum strain are potential sites for microcrack nucleation. (After Muddle, B. C. and Hannink, R. H. J., *J. Am. Ceram. Soc.*, 69, 547, 1986.)

Other crack tip shielding effects:

- decrease of effective elastic modulus

- microcracks degrade process zone material - negative effect
  - fracture surface already available for propagating crack

Influence of particle size on microcrack toughening:
optimum size for maximum toughening effect

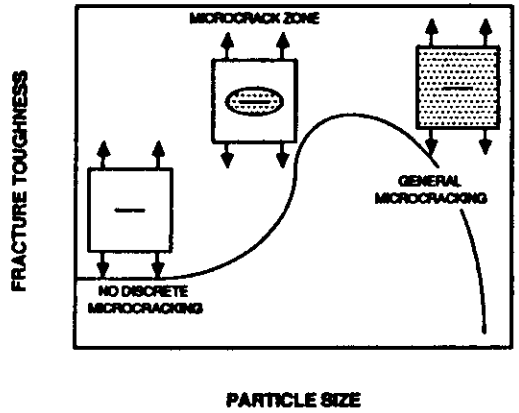

FIGURE 27. Schematic illustration of the effect of particle size on fracture toughness of a microcracking material. For small particles, the critical microcracking stress is too high to form a zone around a crack. As one approaches the critical size, the toughness increases as the zone height increases. At large particle sizes, the material contains microcracks before stressing. (After Evans, A. G. and Faber, K. T., *J. Am. Ceram. Soc.*, 67, 255, 1984.)

CRACK TIP INTERACTIONS

Obstacles in crack path impede crack propagation
- interactions between crack tip stress field and stress concentations / residual stresses associated with obstacles.

Crack bowing

Crack deflection

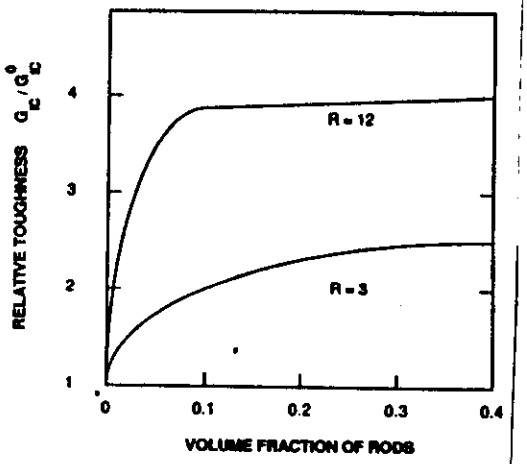

FIGURE 23. The predicted influence of crack deflection on the fracture toughness of a brittle material containing a random array of rod-shaped particles. The influence of increasing the aspect ratio (R) of the rods is included. (After Faber, K. T. and Evans, A. G., *Acta Metall.*, 31, 565, 1983.)

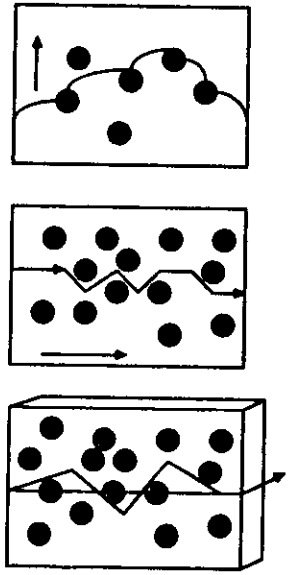

FIGURE 24. A comparison of crack bowing and crack deflection mechanisms. In *a*, a crack front is shown bowing round a set of obstacles. In *b*, the crack path is shown for a crack tilting past obstacles. In *c*, a straight crack front and the twisting it must undergo to avoid a set of obstacles is shown. In each case, the direction of crack propagation is shown with an arrow.

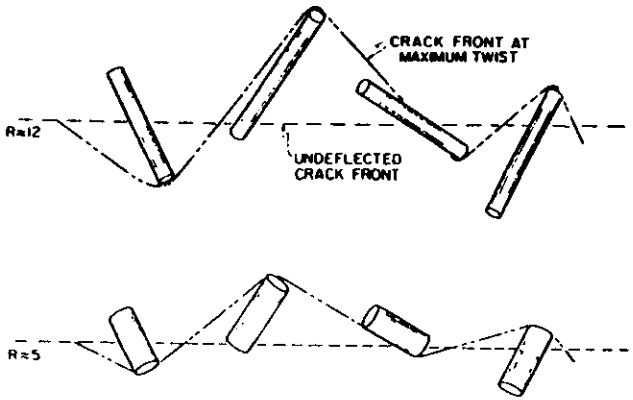

Fig 11. Schematic illustrating the twisting of a crack between rod-shaped particles

WHISKER COMPOSITES

Ref: R. Warren and V. Sarin, *Fracture of whisker reinforced ceramics* To be published in "Applications of fracture mechanics to composite materials", Ed. K. Friedrich, Elsevier.

*SiC, Si_3N_4, Al_2O_4 single crystal whiskers
exceptionally high tensile strength (> E / 100)

* 0.5 - 1.0 μm diameter
100 - 200 μm length

Significant improvement in fracture toughness with 20 - 30 vol% whiskers

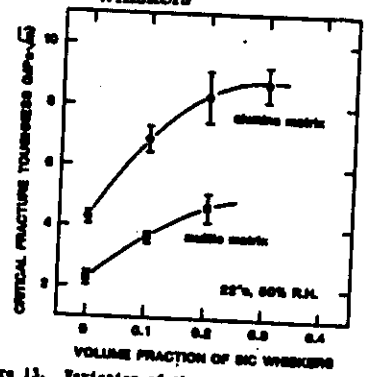

Figure 13. Variation of the toughness of alumina and mullite with volume fraction of SiC whiskers.

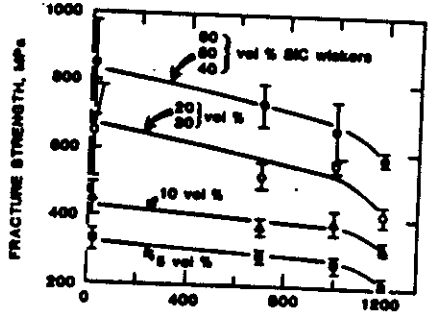

Figure 14. Influence of whisker content on the strength of alumina - silicon carbide whisker materials.

Toughening mechanisms:
- crack bridging
- pull out
- crack deflection
- microcracking

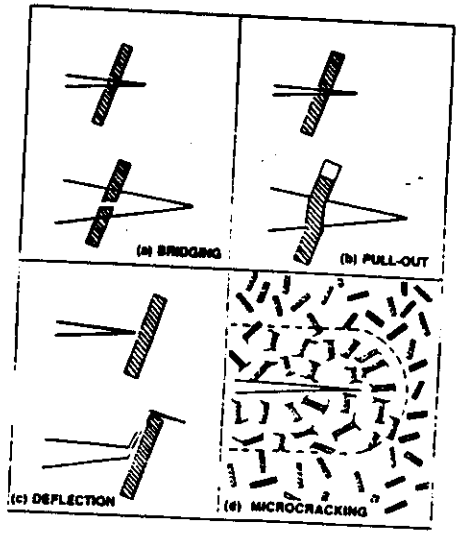

Some proposed toughening mechanisms in whisker reinforced ceramics (note that pull-out of a whisker inclined to the crack plane must involve bending of the whisker (b)).

Crack bridging:

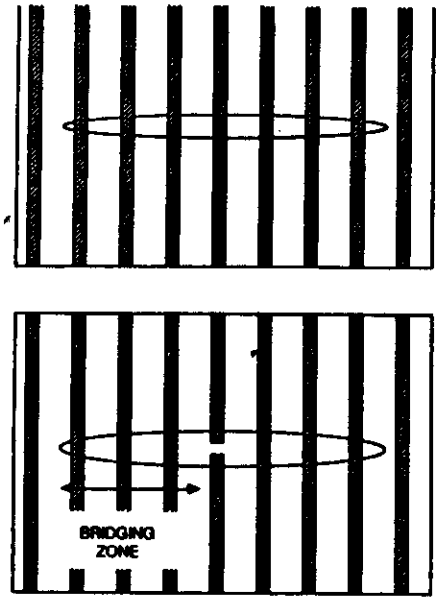

FIGURE 28. Comparison of a crack fully bridged by frictionally bonded fibers with the case where fibers break during matrix cracking forming a bridging zone behind the moving crack front.

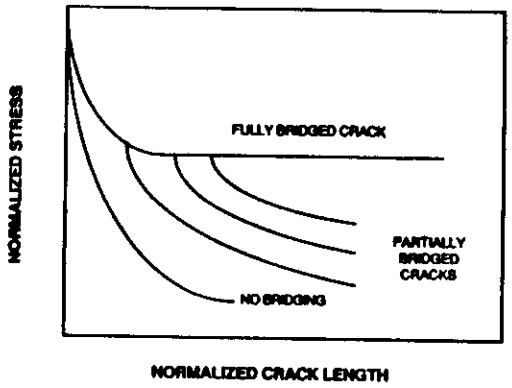

FIGURE 29. The strength of a frictionally bonded, unidirectional fiber composite as a function of crack size. For a fully bridged crack, there is a region where strength does not depend on crack size. For cases where the fibers break during matrix cracking, the strength does depend on crack size and the magnitude of the strengthening depends on the size of the bridging zone. (After Marshall, D. B. and Evans, A. G., *Proc. 5th Int. Conf. on Composite Materials*, Harrigan, W. C., Strife, J., and Dhingra, A. K., Eds., Metallurgical Society, Warrendale, Pa., 1985, 557.)

Pull-out:

- requires a weak whisker / matrix interface
  eg. whiskers coated with graphite

Combined toughening mechanisms:

- different mechanisms are additive and often complement each other.

eg. A whisker unfavourably oriented for pull-out is likely to be favourably oriented for crack deflection.

Room temperature properties of whisker reinforced ceramics:

Table 4. Summary of room temperature properties of whisker reinforced ceramics. Whisker volume fraction is 0.2 unless otherwise stated.

Matrix	Fracture toughness K_{Ic} ($MNm^{-3/2}$)		Fracture strength (MPa)		Weibull modulus, m		Ref.
	matrix	composite	matrix	composite	matrix	composite	
Alumina	3.7	6.7*	510	600	4.6	13.4	65
"	3.7	8.9	-	-			"
"	4.7	9	600	805			14
"	4.7	8.5	520	650			15
"	4.5	8.2	300	550			66
"	5	9.5**	385	650			25
"	5	8.6	385	640			16
Si_3N	7	10.5**	700	500			17
Si_3N_4	7	9.7	700	530			17
"	4.7	4.8	790	720			19
"	6	5	900	600			18
"	-	-	-	-	10	24	67
"	4.7	6.4**	700	975			19
Zirconia	6.2	10	1100	600			68
$MoSi_2$	5.3	8.2	-	-			21
Mullite	2.2	4.6	-	438			14
	2.8	4.4	244	452			15
Cordierite	2.2	3.7	180	260			15
"		4.5	-	360			23
Glass*	1	3.4	100	300			23

* poorer whisker dispersion; ** V_w: 0.3; + Corning 1723, $\alpha = 5.2 \times 10^{-6}\ c^{-1}$

FIBER REINFORCED COMPOSITES

Reference: R. W. Davidge, *Fibre-reinforced ceramics*, Composites, 18 (2) 1987, 92

Semi-continuous fibers C, SiC
often complex composition

Currently available ceramic fibers:

Currently Available Ceramic Fibres

Manufacturer	Designation	Composition	Tensile Strength GPa	Tensile Mod GPa	Density gcm^{-3}	Diameter (μm)
Nippon Carbon	Nicalon	Si(60),C(30),O(10)	2.5-3.5	182-210	2.55	10-20
Avco	SCS-6	SiC(C core)	3.9	406	3.0	140
3M	Nextel 312	Al_2O_3(62),B_2O_3(14) SiO_2(24)	1.7	154	2.7	11
DuPont	FP	-Al_2O_3(99)	1.4	385	3.9	20
Rhone-Poulenc	-	Al_2O_3(85).SiO_2(15)	1.8-2.6	210-250	3.2	9-17
		More recently available fibres				
Ube	Tyrranno	Si, Ti, C, O	3.0	>200	2.4	8-10
Avco		Si, C	2.8	280-315	-	6-10
Dow Corning	MPDC	Si, C, N, O	1.75-2.1	175-210	2.3	10
Celanese	MPZ	Si, C, O, N	2.1-2.6	140-175	2.35	10-15
-	MPS	SiC, O	1.0-1.4	175-210	2.65	10
3M	Nextel 440	Al_2O_3,SiO_2,B_2O_3	2.1	189	3.05	10-12
-	Nextel 480	Al_2O_3,SiO_2,B_2O_3	2.3	224	3.05	10-12
DuPont	PRD-166	Al_2O_3-ZrO_2	2.1-2.6	385	4.2	20

eg. Nicalon (SiC interspersed with SiO_2 and free C) reinforcement of lithium aluminium silicate (LAS) glass ceramic:

Stage I: matrix cracking and load transfer to fibers.

Stage II: reduced modulus - elastic extension of fibers.

Stage III: fiber pull-out.

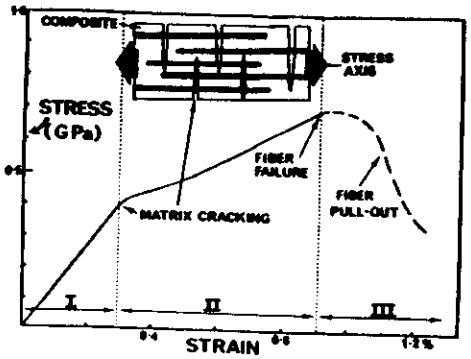

Fig.16. The optimal stress-strain behaviour of a ceramic composite, typified by an LAS glass ceramic containing unidirectional 'Nicalon' SiC fibres

Fabrication of fiber composites

- wide variation of fiber weaves

glass / glass ceramic matrices
- low pressure hot pressing

General difficulty of densification with normal powder processing routes

Infiltration by:

chemical vapour deposition (CVD)
- >1000 °C → 80 - 85 % density
- can make a thin interface coating on woven structure prior to deposition of matrix.
- require interface to be sufficiently strong to allow load transfer from matrix to fibers yet weak enough to fail preferentially prior to fiber failure.

liquid penetration - sol gel routes

Example:

SiC - SiC fiber composite by CVD infiltration
P.J. Lamicq et al. Bull Amer Ceram Soc. 65 (2) 1987, 336

K_{IC} ~ 40 MPa $\sqrt{m}$
- temperature insensitive to 1200 °C
- extreme steep R-curve
- no reduction in strength om thermal shock testing from 1300°C into water

Strength ~ 400 MPa

Problems:
- high temp degadation of fibers
- oxidation / creep response of matrix

Aim: Raise operating temp of this type of composite to 1500-2000 °C

HIGH TEMPERATURE BEHAVIOUR

OXIDATION OF Si_3N_4 CERAMICS

Ref: C. O'Meara, P.H.M. Nilsson & G.L. Dunlop *Oxidation of high performance ceramics based upon* Si_3N_4, Metals Forum 1985 8 194

Si_3N_4 - unstable with respect to oxides

Pure Si_3N_4

high oxygen potentials:

$$Si_3N_4 + 3O_2(g) \rightarrow 3SiO_2(s) + 2N_2(g)$$

SiO_2 forms compact passivating scale.

Low oxygen partial pressures $P_{O_2} < 8 \times 10^{-4}$atm., 1600 K:

$$Si_3N_4 + 3\,SiO_2 \rightarrow 6SiO(g) + 2N_2(g)$$

$$2\,Si_3N_4 + 3O_2(g) \rightarrow 6SiO(g) + 4N_2(g)$$

Parabolic rate law (passivating oxidation)

$$(\Delta/A)^2 = K_p t$$

OXIDATION OF POLYPHASE Si_3N_4

More rapid oxidation than pure Si_3N_4

- influence of intergranular glassy phases and secondary crystalline phases

Glassy phase:

- softens at high temperatures (~1000°C)
  - increased mobility of diffusing species
  - →increased oxidation rate
- contains metallic cations
- continuous with oxide scale
  - difference in composition
- diffusion couple
  - intergranular glass / oxide scale

Rate limiting process for oxidation ?

- outward diffusion of cations ?
- inward diffusion of oxygen ?

Overall oxidation kinetics - parabolic
- NB not because of passivation

D.R. Clarke and F.F. Lange, J Amer Ceram Soc, 1980, 63, 586 :

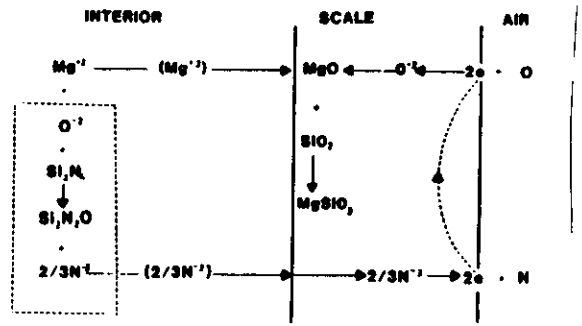

Fig. 3. Schematic diagram illustrating the mechanism for oxidation of MgO-fluxed β-Si_3N_4, proposed by Clarke and Lange [17]

Polyphase oxide scales

Outwards diffusion

→ concentration of cations in oxide scales increases with time
- this effects viscosity / diffusivity of oxide scale
- low melting silicate eutectics

- formation of crystalline phases

cristobalite SiO_2
silicates $Y_2Si_2O_7$
$MgSiO_3$
yttrialite $(H,Na,Fe).(Y,La)_5Si_6O_{21}$
miserite $(Ca,K,Na,Al,Y).SiO_3$

Role of subscalar secondary crystalline phases

Oxidation of secondary crystalline phases
- molar volume changes

Ref: F.F. Lange, Int Met Rev 1980, 25, 1

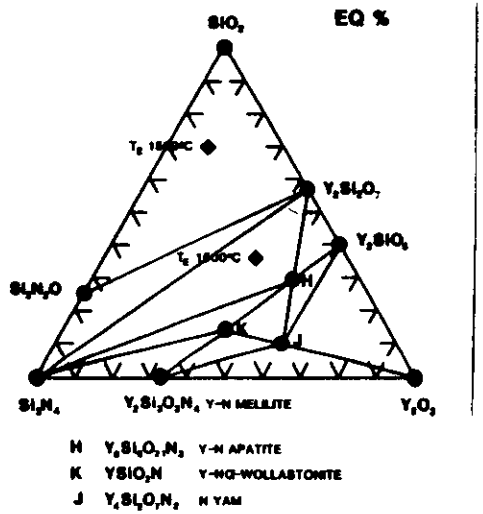

Fig. 4. Behaviour diagram illustrating phase relationships in the Si_3N_4-SiO_2-Y_2O_3 system. After Lange [3]

TABLE 1. Molar Volume Changes upon Oxidation of Secondary Crystalline Phases

Secondary Phase	Oxidation Product	Volume Change %
Y-N melilite ($Y_2Si_3O_3N_4$)	$Y_2Si_2O_7 + SiO_2$	+30*
K-phase ($YSiO_2N$)	$0.5Y_2Si_2O_7$	+12*
Y-N apatite ($Y_4Si_2O_7N_2$)	$1.5Y_{4.67}(SiO_4)_3O + 0.5Y_2Si_2O_7$	+5*
J-phase ($Y_4Si_2O_4N_2$)	$2Y_2SiO_5$	+35†

Avoid: Y-N mellilite; K-phase; J - phase.
→ catastrophic oxidation 900-1200 °C

Good oxidation properties if material fabricated in:

Si_3N_4 - Si_2N_2O - $Y_2Si_2O_7$

and Si_3N_4 - $Y_2Si_2O_7$ - Y,N apatite phase fields

CRYSTALLISATION OF INTERGRANULAR GLASSY PHASE

- during heat treatment
  or high temperature service

Refs: M.H. Lewis, A.R.Bhatti, R.J.Lumby & B.North
J. Matls.Sci, 1980 15 103

L.K.L. Falk & G.L. Dunlop, *Crystallisation of the glassy phase in a S_3N_4 material by post sintering heat treatments*, J. Matls.Sci, 1987 22 4369

Influence of temperature and oxidising environment:

TABLE III Secondary crystalline phases identified by X-ray diffractometry in material heat treated at higher temperatures. α = α-$Y_2Si_2O_7$; β = β-$Y_2Si_2O_7$; W = Y,N-α-wollastonite ($YSiO_2N$); A = Y,N-apatite.

Temperature and time	Depth below oxide scale					
	20–40 μm	100 μm	200 μm	250 μm	400 μm	1.5 mm
1300°C 100 h	α, W					α, W, A
1345°C 125 h	β			β, α, A		
1400°C 7 h	β	β	β, α, W, A		α, W, A	α, W, A

Still have thin intergranular films of glassy phase after full crystallisation.

Crystallisation to appropriate secondary crystalline phases can lead to considerably improved oxidation and creep properties

eg. B.S.B Karunaratne & M.H. Lewis J. Matls Sci. 1980 15 449

HIGH TEMPERATURE MECHANICAL BEHAVIOUR

Refs:

1. W.R. Cannon & t.G. Langdon *Creep of ceramics*
   I. J Matls Sci 1983 18 1
   II. ibid 1988 23 1

2. J.E.Marion, A.G. Evans, M.D.Drory; & D.R.Clarke *High temperature failure initiation in liquid phase sintered materials* Acta Met 1983 31 1445

3. A. G. Evans & A. Rana *High temperature failure mechanisms in ceramics* Acta Met 1980 28 129

4. A. G. Evans & W. Blumenthal *High temperature failure in ceramics* in "Fracture mechanics of ceramics" Eds R.C.Bradt et al. Plenum NY 1983 p.4

5. F.F.Lange *High temperature deformation and failure phenomena of polyphase Si_3N_4 materials* in "Progress in nitrogen ceramics" Ed F.L Riley, Martinus Nijhoff Publishers 1983 p467

6. B.S.B Karunaratne & M.H. Lewis *High temperature fracture and diffusional deformation mechanisms in SiAlON ceramics* J. Matls Sci. 1980 15 449

Creep equation:

$$\dot{\varepsilon} = AGb/kT\,(b/d)^p(\sigma/G)^n\,D_o\exp(-Q/RT)$$

PHARR and ASHBY: ON LIQUID-ENHANCED CREEP

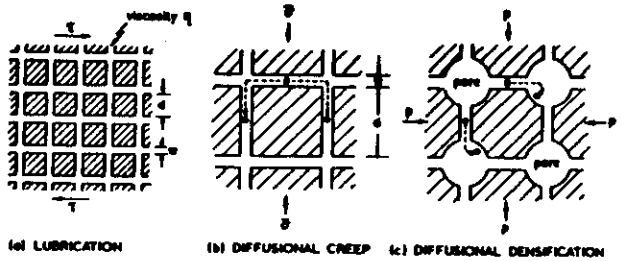

Fig. 11. Mechanisms for liquid-enhanced creep.

n = 1 Newtonian viscous

Diffusion creep:

Nabarro-Herring	p = 2	Q_l
Coble	p = 3	Q_{gb}

Lubricated flow p = 1
Solution precipitation
(Pharr & Ashby Acta Met 1983 31, 129

n = 2 Extensive grain boundary sliding
(eg superplasticity)

n = 2 Dislocation creep
- seldom of importance to high strength ceramics

Creep of Si_3N_4 materials:

Dominated by **glassy phase.**

Steady state creep generally by solution / precipitation
(small transient strains by viscous flow)

Cavitation also contributes to total strain

Influence of oxidation / crystallisation

Lange:

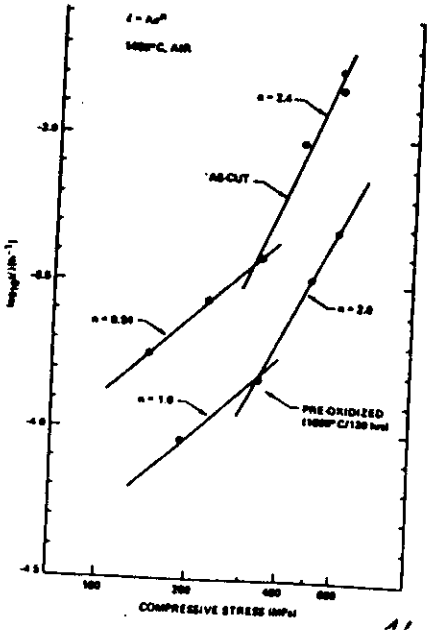

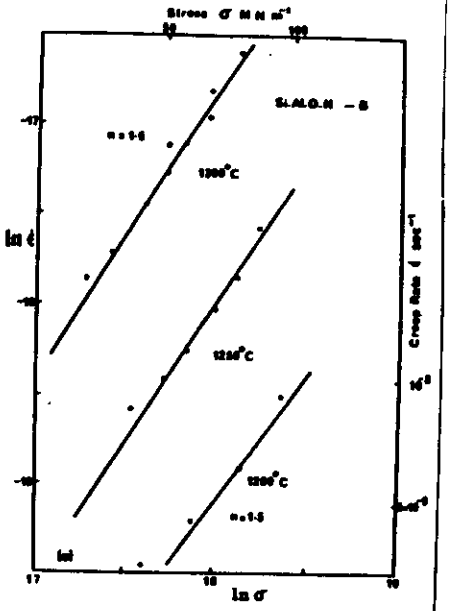

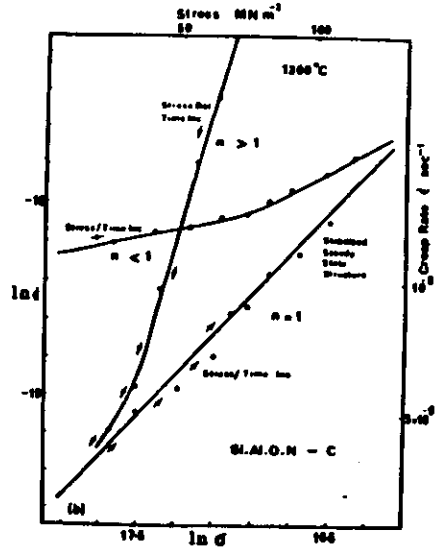

Figure 3 (a) Stress-exponents (n) for creep of ceramic B at various temperatures determined from incremental stress tests (open and closed circles at 1300° C are for two separate specimens. (b) Non-steady-state behaviour illustrated in determining values for n for ceramic C with increasing or decreasing stress increment (upper curves). The value of $n = 1$ characteristic of diffusional creep is obtained after long test times or for pre-heat treated specimens.

Karunaratne + Lewis

Lewis

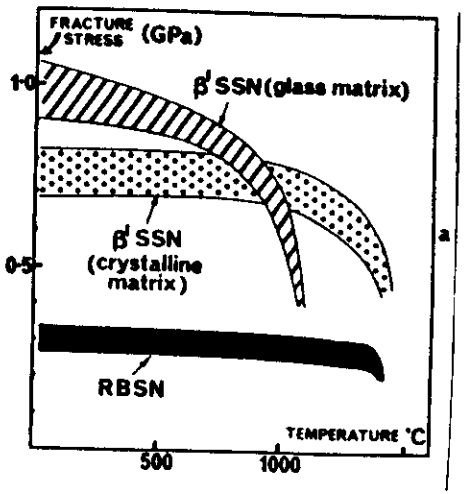

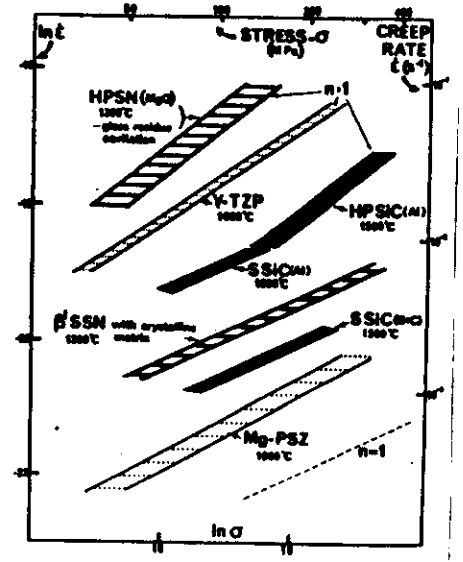

Fig. 9. A comparison of pseudo-steady-state creep rates for a range of Si-based and ZrO_2-toughened ceramics within differing temperature intervals. The stress-exponent (n) of the creep rate is frequently=1, indicative of a diffusion-controlled mechanism.